PITTING DAMAGE LEVELS ESTIMATION FOR PLANETARY GEAR SETS BASED ON MODEL SIMULATION AND GREY RELATIONAL ANALYSIS

Cheng Zhe[1], Hu Niaoqing[1], Gu Fengshou[2], Qin Guojun[1]
[1] *Key Laboratory of Science and Technology on Integrated Logistics Support, National Univ. of Defense Technology, Changsha, P.R.China*
[2] *University of Huddersfield, Huddersfield, UK*
E-mail: chengzhenudt@163.com; hnq@nudt.edu.cn

Received Month 0000, Accepted Month 0000
No. 00-CSME-00, E.I.C. Accession Number 0000

ABSTRACT

The planetary gearbox is a critical mechanism in helicopter transmission systems. Tooth failures in planetary gear sets will cause great risk to helicopter operations. A gear pitting damage level estimation methodology has been devised in this paper by integrating a physical model for simulation signal generation, a three-step statistic algorithm for feature selection and damage level estimation for grey relational analysis. The proposed method was calibrated firstly with fault seeded test data and then validated with the data of other tests from a planetary gear set. The estimation results of test data coincide with the actual test records, showing the effectiveness and accuracy of the method in providing a novel way to model based methods and feature selection and weighting methods for more accurate health monitoring and condition prediction.

Keywords: planetary gear sets; pitting damage; feature selection; grey relational analysis; damage level estimation.

TITRE FRANÇAIS DE L'ARTICLE (MAXIMUM DEUX LIGNES)

RÉSUMÉ

Le résumé français est obligatoire. Évidement, si l'article est rédigé en français, le titre principal et le résumé principal sont en français. Par contre, il ne faut pas traduire le texte « Received…Accession Number 0000 ».

Mots-clés : premier mot-clé; deuxième mot-clé; troisième mot-clé.

NOMENCLATURE

b	clearance constant
b_{rpi}	external meshing side clearance (m)
b_{spi}	internal meshing side clearance (m)
C	mesh damping constant (N/m^2)
c	depth parameter of pitting damage (mm)
C_{rpi}	mesh damping between ring gear and planet gear (N/m^2)
C_{spi}	mesh damping between sun-gear and planet gear (N/m^2)
D	adhesive engaging force (N)
f_0	mesh frequency of sun gear (Hz)
f_d	rotary frequency of sun gear (Hz)
I	rotational inertia ($kg \cdot m^2$)
J	number of operation conditions
K_{rpi}	mesh stiffness between ring gear and planet gear (N/m)
K_{spi}	mesh stiffness between sun-gear and planet gear (N/m)
M	equivalent mass (kg)
m	mass (kg)
$\bar{m}$	modulus (mm)
N	number of planet gears
P	elastic engaging force (N)
p	pitch of tooth (mm)
r	relational coefficient
r_b	radius of basic circle (m)
S	standard deviation
s	severity of tooth damage (%)
T_D	driving torque (N·m)
T_L	loading torque (N·m)
w	weight of feature
z	classification distance

Greek symbols

α	mesh angle (deg)
β	distinguishing coefficient
γ	grey relational grade
η	grey relational coefficient

Subscripts

c	carrier
p	planet gear
r	ring gear
s	sun gear

1. INTRODUCTION

The majority of mishaps in helicopters are caused by engine and drive train failures. To reduce these mechanically induced failures and excessive maintenance, it is vital to accurately identify and diagnose developing faults in the mechanical system. Planetary gear sets are common mechanical components and are widely used to transmit power and change speed and/or direction in rotary aircrafts. One of the most common causes of planetary gear sets failure is tooth defect due to excessive stress conditions. It results in progressive damage to gear teeth and ultimately leads to the complete failure of the planetary gear sets. This fault is particularly challenging as it is located deep inside the main transmission, suggesting it would be difficult to detect earlier.

Because of the high importance and challenge, the subject of damage level estimation for planetary gear sets has been studied intensively and resulted in a number of advanced papers published in several key journals and at conferences. In general, methods reported in these papers could be viewed through two categories: data-driven approach and model-based approach. Coppe [1] presented a simple model from the assumption that for each combination of crack location and inspector there is a threshold crack size such that all cracks above this size will be detected and all below that size will be missed. The proposed model adjusts the threshold crack size according to the difficulty associated with the crack location and the competence of inspectors. Choi [2] developed a method to estimate the size of a tooth transverse crack for a spur gear in operation. Using gear vibrations measured from an actual gear accelerated test, this study examined existing gear condition indices to identify those which correlated well to crack size and established their utility for crack size estimation through index fusion using a neural network. Ma [3] developed a model-based demodulation scheme to exploit the information contained in wideband gear vibrations and compared it to a state of the art technique that uses a vibration average of a gear with two defects of different sizes. Lei and Zuo [4] proposed a method to classify the different levels of gear cracks automatically and reliably. The proposed method is applied to identifying the gear crack levels and the results obtained demonstrate the effectiveness of the method.

In general, the data-driven methods aforementioned provide little guarantee of their estimation accuracy. Moreover, they are usually vague about the relationship between the index and damage severity since they assume some kind of simple black-box model. On the other hand, the physical-based approach has high computational costs associated with the physical models and these methods are only suitable for off-line applications. In addition, the datasets used for the damage severity estimation of planetary gear sets is interfered strongly with environmental noise and many frequency components of other moving parts and the damage feature information is totally different from the ordinary gear train. Thus the feature selection is another challenge to be faced in this field.

In this paper, a novel damage severity estimation method is presented for 2K-H planetary gear sets based on a hybrid approach which is composed of an analytical model for dynamic response and damage feature information analysis, a three-step statistic algorithm for feature selection and weighting and a grey relational analysis algorithm for damage level estimation. The rest of the content will address the method development according to these three phases.

2. PHYSICAL MODEL OF PLANETARY GEARS WITH DAMAGE

Modeling of the gear tooth failure can help to analyze this dynamic change in order to give suitable tools to diagnose such failures. Whilst the modeling of healthy gear systems nowadays is extensively carried out, the failure modeling is still subject to many research papers. Gear tooth failures are generally assessed by the determination of the tooth stiffness reduction. The finite elements method is the most frequently used technique to do this [5–8], but it requires, in certain applications, mesh refinements and then much computations time. Analytical methods can be a good alternative to model tooth failures. Some literature focuses on the tooth stiffness reduction due to damage by considering qualitative proportional reduction [9–14]. This research is based on the analytical method.

2.1. Physical Model of Healthy Planetary Gear set

The epicyclic stage of the transmission is more complex due to its multiple components and the orbital motion of the planets. Noting that the stiffness of the planet gear support is very rigid and the internal ring gear is fixed to the top of the transmission casing, the central displacement of planet-gears and ring gear is ignored to simplify the model of 2K-H planetary gear sets. Then a lumped parameter, pure torsional dynamical formulation is employed to develop the physical model of 2K-H planetary gear sets. As shown in Fig.1, K_{spi} denotes mesh stiffness between sun-gear and planet gear; K_{rpi} denotes mesh stiffness between planet gear and ring gear; C_{spi} denotes mesh damping between sun-gear and planet gear; C_{rpi} denotes mesh damping between planet gear and ring gear. θ_s, θ_{pi} and θ_c denote the rotation angle of sun-gear, planet gear and carrier respectively. T_D, and T_L denote driving torque and loading torque respectively. s, r, p*i* and c are the subscripts denoting sun-gear, ring gear, the *i*th planet gear and carrier. By ignoring mesh errors and defining internal meshing side clearance and external meshing side clearance as $2b_{spi}$ and $2b_{rpi}$, respectively, the adhesive engaging force D and the elastic engaging force P are represented as:

$$\begin{cases} D_{spi} = C_{spi}(\dot{\theta}_s r_{bs} - \dot{\theta}_{pi} r_{bpi} - \dot{\theta}_c r_c \cos\alpha) \\ D_{rpi} = C_{rpi}(\dot{\theta}_{pi} r_{bpi} - \dot{\theta}_c r_c \cos\alpha) \\ P_{spi} = K_{spi}(t) f(\theta_s r_{bs} - \theta_{pi} r_{bpi} - \theta_c r_c \cos\alpha, b_{spi}) \\ P_{rpi} = K_{rpi}(t) f(\theta_{pi} r_{bpi} \quad \theta_c r_c \cos\alpha, b_{rpi}) \end{cases} \tag{1}$$

where $K(t)$ is time varying mesh stiffness, C is mesh damping constant and r_b is radius of basic circle, $f(x,b)$ is nonlinear clearance function defined by:

$$f(x,b) = \begin{cases} x-b & (x > b) \\ 0 & (-b \le x \le b) \\ x+b & (x < -b) \end{cases} \tag{2}$$

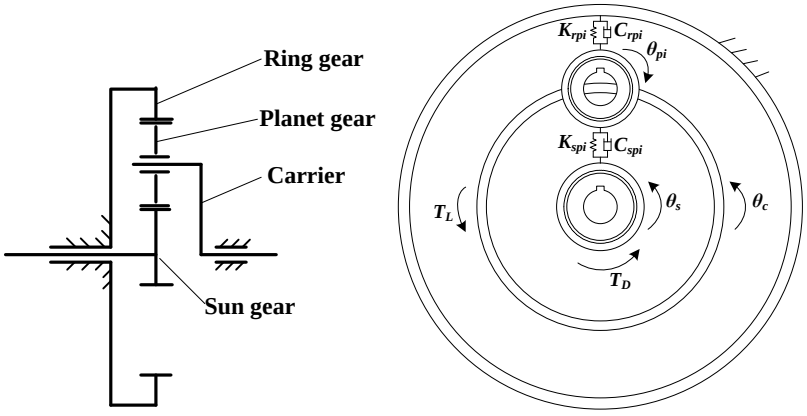

Fig. 1. Pure torsional model of 2K-H planetary gear sets.

Dynamical differential equations of 2K-H planetary gear sets could be deduced from Lagrange equations:

$$\begin{cases} I_{\mathrm{s}}\ddot{\theta}_{\mathrm{s}} + \sum_{i=1}^{\mathrm{N}}(D_{\mathrm{sp}i} + P_{\mathrm{sp}i})r_{\mathrm{bs}} = T_{\mathrm{D}} \\ I_{\mathrm{p}i}\ddot{\theta}_{\mathrm{p}i} - (D_{\mathrm{sp}i} - D_{\mathrm{rp}i} + P_{\mathrm{sp}i} - P_{\mathrm{rp}i})r_{\mathrm{bp}i} = 0 \\ \left(I_{\mathrm{c}} + \sum_{i=1}^{\mathrm{N}} m_{\mathrm{p}i}r_{\mathrm{c}}^2\right)\ddot{\theta}_{\mathrm{c}} - \sum_{i=1}^{\mathrm{N}}(D_{\mathrm{sp}i} + D_{\mathrm{rp}i} + P_{\mathrm{sp}i} + P_{\mathrm{rp}i})r_{\mathrm{c}}\cos\alpha = T_{\mathrm{L}} \end{cases} \tag{3}$$

where I is rotational inertia of the subcomponents, m is mass, α is mesh angle and N is the quantity of planet-gears.

The equations above are positive semi-definite, nonlinear equations, which have N+2 degrees-of-freedom (DOF's), with angle displacements of rigid bodies in a coordinated system. For translating angle displacements of rigid bodies into relative linear displacement, the relative displacements between sun-gear and planet gear $x_{\mathrm{sp}i}$, and the relative displacement between sun-gear and carrier x_{sc} are defined as:

$$\begin{cases} x_{\mathrm{sp}i} = \theta_{\mathrm{s}}r_{\mathrm{bs}} - \theta_{\mathrm{p}i}r_{\mathrm{bp}i} - \theta_{\mathrm{c}}r_{\mathrm{c}}\cos\alpha \\ x_{\mathrm{sc}} = \theta_{\mathrm{s}}r_{\mathrm{bs}} - 2\theta_{\mathrm{c}}r_{\mathrm{c}}\cos\alpha \end{cases} \tag{4}$$

After this, equivalent mass is supposed as M, $M = I / r_b^{\,2}$, $M_{\mathrm{c}} = I_{\mathrm{c}} / r_{\mathrm{bc}}^{\,2} + \sum_{i=1}^{\mathrm{N}} m_{\mathrm{p}i} / \cos^2\alpha$.

Substituting Eq. (1) and Eq. (3) into Eq. (4) and simplifying the equations obtained, then the dynamic model of planetary gear sets is represented as:

$$\begin{cases} \ddot{x}_{\mathrm{sp}i} + \sum_{i=1}^{\mathrm{N}}\left[\left(\frac{1}{M_{\mathrm{s}}} + \frac{1}{M_{\mathrm{c}}}\right)C_{\mathrm{sp}i}\dot{x}_{\mathrm{sp}i} + \frac{1}{M_{\mathrm{c}}}C_{\mathrm{rp}i}\left(\dot{x}_{\mathrm{sc}} - \dot{x}_{\mathrm{sp}i}\right)\right] + \frac{1}{M_{\mathrm{p}i}}\left[C_{\mathrm{sp}i}\dot{x}_{\mathrm{sp}i} - C_{\mathrm{rp}i}\left(\dot{x}_{\mathrm{sc}} - \dot{x}_{\mathrm{sp}i}\right)\right] \\ + \sum_{i=1}^{\mathrm{N}}\left[\left(\frac{1}{M_{\mathrm{s}}} + \frac{1}{M_{\mathrm{c}}}\right)K_{\mathrm{sp}i}(t)\,f\left(x_{\mathrm{sp}i}, b_{\mathrm{sp}i}\right) + \frac{1}{M_{\mathrm{c}}}K_{\mathrm{rp}i}(t)\,f\left(x_{\mathrm{sc}} - x_{\mathrm{sp}i}, b_{\mathrm{rp}i}\right)\right] \\ + \frac{1}{M_{\mathrm{p}i}}\left[K_{\mathrm{sp}i}(t)\,f\left(x_{\mathrm{sp}i}, b_{\mathrm{sp}i}\right) - K_{\mathrm{rp}i}(t)\,f\left(x_{\mathrm{sc}} - x_{\mathrm{sp}i}, b_{\mathrm{rp}i}\right)\right] = \frac{T_{\mathrm{D}}}{M_{\mathrm{s}}r_{\mathrm{bs}}} + \frac{T_{\mathrm{L}}}{M_{\mathrm{c}}r_{\mathrm{c}}\cos\alpha}; \\ \ddot{x}_{\mathrm{sc}} + \left(\frac{1}{M_{\mathrm{s}}} + \frac{2}{M_{\mathrm{c}}}\right)\sum_{i=1}^{\mathrm{N}}C_{\mathrm{sp}i}\dot{x}_{\mathrm{sp}i} + \frac{2}{M_{\mathrm{c}}}\sum_{i=1}^{\mathrm{N}}\left[C_{\mathrm{rp}i}\left(\dot{x}_{\mathrm{sc}} - \dot{x}_{\mathrm{sp}i}\right)\right] + \left(\frac{1}{M_{\mathrm{s}}} + \frac{2}{M_{\mathrm{c}}}\right)\sum_{i=1}^{\mathrm{N}}K_{\mathrm{sp}i}(t)\,f\left(x_{\mathrm{sp}i}, b_{\mathrm{sp}i}\right) \\ + \frac{2}{M_{\mathrm{c}}}\sum_{i=1}^{\mathrm{N}}K_{\mathrm{rp}i}(t)\,f\left(x_{\mathrm{sc}} - x_{\mathrm{sp}i}, b_{\mathrm{rp}i}\right) = \frac{T_{\mathrm{D}}}{M_{\mathrm{s}}r_{\mathrm{bs}}} + \frac{2T_{\mathrm{L}}}{M_{\mathrm{c}}r_{\mathrm{c}}\cos\alpha}. \end{cases} \tag{5}$$

2.2. Physical Model of Planetary Gears with Tooth Pitting

Two stage planetary gear sets are usually used in the main transmission of a helicopter, the second stage is subjected to a much greater loading than the first stage and consequently the oil film on gear meshing space always breaks or is hard to form at this stage. As a result, high temperature adhesion and fatigue contact stress will occur easily between gear mesh surfaces, the metal surface will tear off and appear pit injury on the tooth surface. This injury is called pitting.

In this paper, pitting on the sun gear tooth surface is considered. To simplify the model of pitting, at each section of the tooth, the shape of pitting is approximated with straight lines according to [10], the width *a*, length *b*, the depth *c* and the distance to the tooth top *d* as shown in Fig.2 (a). The pitch of teeth is *p*, modulus of gear is $\bar{m}$, then $p = \pi\bar{m}$. The severity of pitting is defined as *s*, that is determined by the depth parameter *c* i.e. $s = s(c)$ but not considering the effect of parameters *a*, *b*, *d* to the severity of pitting in this research. For simplifying the dynamical model of planetary gear sets, define the depth of pitting as $\tilde{c}_i = \frac{5c_i}{p/2} = \frac{5c_i}{\pi\bar{m}/2} = \frac{10c_i}{\pi\bar{m}}$, $i = 1,2,3...$, $\tilde{c}_i \in [0\%, 100\%]$ and then, $s_i = s(\tilde{c}_i)$, $s_i \in [0\%, 100\%]$. The tooth and gear mesh stiffness of the gear pair, which is composed by sun-gear and planet-gear, is calculated by taking into account the geometric changes due to the tooth pitting as illustrated in Fig. 2. The detailed procedure to calculate mesh stiffness can be found in Reference [9,10].

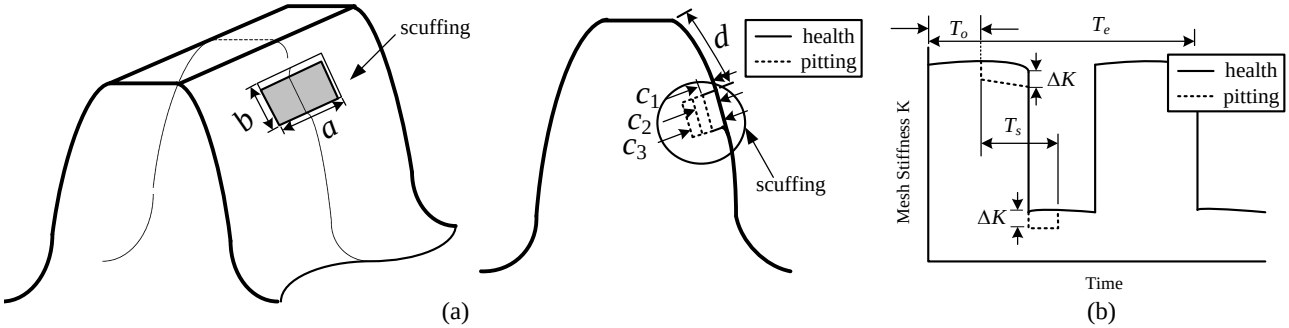

Fig. 2. The view of damage gear tooth and its meshing stiffness's variation. (a) Lateral and axial view of damage gear tooth, (b) Response of meshing stiffness to pitting damage.

Referring to Fig. 2(b), gear mesh stiffness evolution caused by sun gear tooth pitting is defined as $\Delta K(s, f_s, t)$, so the time varying mesh stiffness with sun gear tooth breakage is given by:

$$\begin{cases} K_{spi}(t) = K_0(f_0, t) + \Delta K(s, f_s, t) \\ |\Delta K| = g(s) \end{cases} \tag{6}$$

where $K_0(f_0, t)$ is the mesh stiffness of gear pair in a healthy case, f_0 and f_d is the mesh frequency of planetary gear set and the rotary frequency of sun gear. The dynamical model of 2K-H planetary gear set with sun gear tooth pitting is acquired by substituting Eq. (6) into Eq. (5).

2.3. Simulation of Physical Models

To obtain a deep understanding of the dynamics described with the equations, the four-order Runge-Kutta method is selected for numerical solutions in Matlab 7.0. The parameters are set up according to Table 1. The duration and step size in solving the equations is set to 1 second and 0.0001 second respectively.

Table 1. Parameters value in the models.

Parameter Name (Unit)	Value	Parameter Name (Unit)	Value
Modulus (mm)	2.5	Tooth Width (mm)	12
Tooth Number of Sun Gear	28	Pressure Angle (Deg)	20

Parameter Name (Unit)	Value	Parameter Name (Unit)	Value
Tooth Number of Planet Gear	32	Driving Torque (N•m)	100
Tooth Number of Ring Gear	92	Loading Torque (N•m)	220
Number of Planet Gear	4	Material	40Cr

Fig. 3 shows typical dynamic responses in both the time domain and the frequency domain which are registered on the internal ring gear for a healthy planetary gear set and 3 different levels of pitting. The healthy case is characterized by the dominance of the gear mesh frequency, denoted by 1X and its harmonics of 2X, 3X etc. For pitting case, amplitude modulation of the gear mesh signal by the defect signal is clearly observed, which occurs once a revolution. As a consequence, many new frequency components appear at the sides of the dominant frequency. It can be seen that the amplitude of new frequency components increases with the growth of pitting severity. These features are very close to experimental observations in the previous study literatures [13,14].

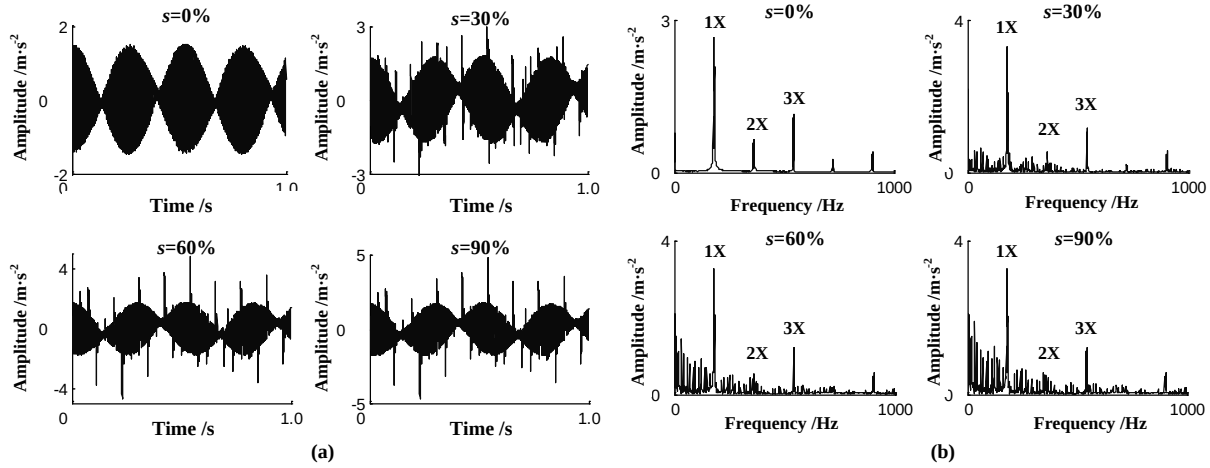

Fig. 3. Simulation signals in (a) time domain & (b) frequency domain.

3. FEATURE SELECTION AND WEIGHTING

From literature review, 27 features have found in different cases of gearbox condition monitoring. In this study they are all explored to obtain an optimal subset for the detection and damage severity estimation in planetary gear sets and organized into four groups and assigned with serial numbers.

(1) Features derived from the time domain are used most frequently in gearbox diagnosis [15]. They include root mean squared(RMS), crest factor(CF), energy ratio(ER), kurtosis, standard deviation, energy operator, absolute mean value, clearance factor and impulse factor, which are assigned with serial numbers 1 to 9 respectively for the ease of identification in the process of feature selection.

(2) There are many other traditional statistical feature parameters for damage detection, such as FM0, FM4, NA4, M6A, M8A, NB4, NA4*, NB4*, M6A* and M8A*, generally used in planetary gearbox condition monitoring [16]. The serial numbers of these features are 10 to 19.

(3) Other kinds of feature parameters based on frequency spectrum of vibration signal are widely used to detect and diagnose faults in helicopter power trains [17,18], such as mean frequency(MF), frequency centre(FC), root mean square frequency(RMSF) and standard deviation frequency(STDF). The serial numbers of these features are 20 to 23.

(4) Other than the features presented above, there are some important features which have been validated in literature, which are named Intra-Revolution Energy Variance(IREV)[19], Spectrum Kurtosis(SK)[20,21], local spectrum kurtosis[22], NSR[23]. The serial numbers of these features are 24 to 27.

Each of the simulation signals generated by the dynamical models is processed to obtain these feature parameters.

3.1. Feature Selection

Damage severity estimation consists of two stages: damage detection and damage level identification. An optimal feature suitable for damage severity estimation should have three merits: the first one is sensitivity, which means that the feature has a wider classification distance; the second one is stability, which means that the feature has same classification performance in different operation conditions (including loading and rotational speed); the last one is relational, which means the feature is closely related to the damage evolution. In this research, target features were selected from the 27 feature parameters above. A statistic algorithm named two-sample Z-test is commonly used to measure the distance of a two class case [19,22]. In this research, this algorithm is applied as sensitivity analysis algorithm, and then it is modified to analyze the stability and relationality of the features. The feature selection procedure can be described as follows:

(1) Sensitivity analysis: For the *i*th feature parameter, calculating the classification distance of the healthy samples and the fault seeded samples in the same condition by two samples z-test procedure:

$$z_i = \frac{\left|\overline{\mathbf{X}}_{i,1} - \overline{\mathbf{X}}_{i,2}\right|}{\sqrt{\frac{S^2_{\mathbf{X}_{i,1}}}{n_1} + \frac{S^2_{\mathbf{X}_{i,2}}}{n_2}}} \tag{7}$$

where $\mathbf{X}_1$ and $\mathbf{X}_2$ are the healthy sample set and the fault seeded sample set, $S_{\mathbf{X}}$ and $\overline{\mathbf{X}}$ are the standard deviation and mean of $\mathbf{X}$, respectively, and n is the sample number for each sample set. $i = 1, 2, ..., \mathrm{I}$, I is the number of feature parameters above.

(2) Stability analysis: The classification distance of the *i*th feature parameter of jth condition is $z_{i,j}$, $j = 1, 2, ..., \mathrm{J}$. Calculating the similarity ratio of classification distance for different condition:

$$s_i = \frac{S_{\mathbf{Z}_i} / \sqrt{n_{z_i}}}{\sum_{m=1,n=1}^{\mathrm{J}} \left|z_{i,m} - z_{i,n}\right|} \tag{8}$$

where $\mathbf{z}_i$ is the classification distance vector of the *i*th feature parameter for different conditions, $S_{\mathbf{Z}_i}$ is the standard deviation of $\mathbf{z}_i$, J is the number of conditions and n is the element number of $\mathbf{z}_i$. A higher value of s means that the feature can differentiate between damage conditions with better performance.

(3) Relational analysis: In this paper, whether a feature is closely related to the damage is based on the performance of tracing damage. Only the feature be monotonic and close to the damage evolution curve, it could be suggested as a better indicator in tracing damage. To

analyze the performance of damage tracing quantitatively, we define damage severity curve as a step curve, as be shown in Fig. 4. Based on the consistency check between feature curve (real line) and damage severity step curve (dashed line), the performance of damage tracing could be evaluated quantitatively.

$$r_i = \frac{\sqrt{\frac{S^2_{\mathbf{X}_{i,1}}}{n_1} + \frac{S^2_{\mathbf{X}_{i,2}}}{n_2}}}{\left|\bar{\mathbf{X}}_{i,1} - \bar{\mathbf{X}}_{i,2}\right|} \tag{9}$$

It is clear that a larger z_i and s_i suggests that the corresponding features have a better performance in sensitivity and stability in damage detection. A larger r_i means that the corresponding features are more relational to the damage evolution. Thus a feature can be selected to estimate damage severity from the potential feature set when these three criteria are above a predefined threshold for feature selection.

3.2. Feature Selection

A feature weighing method is often used to integrate different features for effective fault classification. After a subset of feature is selected, the weight of each selected feature is determined according to the relevance with damage evolution. As shown by the Eq. (10), the value of r_i reflects the relevance ratio of the *i*th feature with damage evolution. It means that a larger value of r_i reflects a higher degree of relevance and hence more correlation to the evolution process to be explored. As the result of that, the *i*th feature could be given a high weight, the relation of *r* and *w* could be interpreted as:

$$\begin{cases} w_1 / r_1 = w_2 / r_2 = \ldots = w_i / r_i = \ldots = w_n / r_n \\ w_1 + w_2 + \ldots + w_i + \ldots + w_n = 1 \end{cases} \tag{10}$$

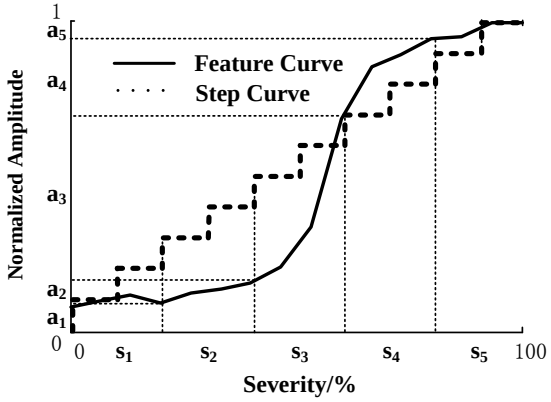

Fig. 4. The feature curve and the step curve of damage evolution.

4. DAMAGE LEVEL ESTIMATION BASED ON GRA

4.1. Grey Relational Analysis for Damage

In grey theory, grey relational analysis (GRA) is often used to find a solution for a problem with limited information reckoned. As it is applied to analyze stochastic variables, the damage in planetary gear sets could be identified based on the relational analysis of an unknown mode

and a normal mode. Before damage relational analysis, a normal damage mode matrix should be created as:

$$\mathbf{X}_{0i}(k)=\begin{bmatrix} X_{0i}(1) & \cdots & X_{0i}(\mathrm{K}) \end{bmatrix} \begin{bmatrix} X_{01}(1) & X_{01}(2) & \cdots X_{01}(k)\cdots & X_{01}(\mathrm{K}) \\ X_{02}(1) & X_{02}(2) & \cdots X_{02}(k)\cdots & X_{02}(\mathrm{K}) \\ \vdots & \vdots & \vdots & \vdots \\ X_{0i}(1) & X_{0i}(2) & \cdots X_{0i}(k)\cdots & X_{0i}(\mathrm{K}) \end{bmatrix} \tag{11}$$

where K is the number of severity level, k=2 for detecting damage, and k>=3 for identifying the level of damage, detection accuracy increases as the increment of k. i is the feature parameter number in each normal mode. Define the feature vector of unknown signal as $\mathbf{X}_i(j)=[X_1(j),X_2(j),\ldots,X_i(j)]^{\mathrm{T}}$, $j\in\{1,2,\ldots,\mathrm{K}\}$, j is damage level number of unknown signal. Grey relational coefficient (GRC) is expressed as:

$$\eta_i(k)=\frac{\min\limits_i\min\limits_k A_i(k)+\beta\max\limits_i\max\limits_k A_i(k)}{A_i(k)+\beta\max\limits_i\max\limits_k A_i(k)} \tag{12}$$

where $A_i(k)=\left|X_{0i}(k)-X_i(j)\right|$, $\eta_i(k)$ is the grey relational coefficient of $X_{0i}(k)$ and $X_i(j)$; β is the distinguishing coefficient, usually $\beta=0.5$. Supposing γ_{ij} as the grey relational grade (GRG) of $X_i(j)$ and $X_{0i}(k)$, then

$$\gamma_{j0}(k)=\frac{1}{\mathrm{I}}\sum_{i=1}^{\mathrm{I}}\eta_i(k) \tag{13}$$

where I is the number of features.

4.2. Damage Level Estimation

Generally, the ideal aim of damage severity estimation is to determine the severity of damage accurately, but as there are many uncertain factors in sensing signals, it is difficult or even impossible to yield the deterministic value of damage severity. As a result of that, it would be more feasible to estimate the damage levels.

After selection and weighting, the feature parameter set used for damage level estimation is marked as $\overline{\mathbf{F}}=\{F_1,F_2,...,F_i,...,F_{\mathrm{I}}\}$, and the weight set of the corresponding feature parameter set is $\overline{\mathbf{W}}=\{W_1,W_2,...,W_i,...,W_{\mathrm{I}}\}$, I is the number of feature parameters in the set. The feature parameter set and the weight set are used to carry out GRA for damage level estimation.

In this research, simulation signals of different damage levels are acquired from the damage seeded models. Then calculating the feature parameters $\overline{\mathbf{F}}$ of simulation signals and forming the normal damage mode matrix $\mathbf{F}_{0i}(k)$, k is the damage level number of simulation signals.

The test signal to be detected and estimated is labeled as s, and the feature vector of s is $\mathbf{F}_i(s)$. Using Eq. (12) and Eq. (13) to calculate the GRC of $\mathbf{F}_{0i}(k)$ and $\mathbf{F}_i(s)$, and then the GRG is calculated by:

$$\gamma_{j0}(k)=\frac{1}{I}\sum_{i=1}^{I}\eta_i(k)W_i \tag{14}$$

Following this a GRG vector $\boldsymbol{\gamma}_{j0} = (\gamma_{j0}(1), \gamma_{j0}(2), ..., \gamma_{j0}(k), ..., \gamma_{j0}(\mathrm{K}))$ is obtained, and the level number k of $\max[\gamma_{j0}(k)]$ is the damage level of $\mathbf{X}_i(j)$.

5. TEST VALIDATION

5.1. Helicopter Transmission Test Rig

The model configuration is based upon the second stages of a planetary gearbox in a helicopter transmission test rig. As shown in Fig.5, it has three different types of gear transmission systems. The first system consists of a spur-bevel gear pair. The horizontal input shaft holds an 18-tooth spiral-bevel pinion which drives a 36-tooth spur-bevel gear on the vertical intermediate shaft. The second system is a planetary gearbox, which consists of two 2K-H planetary gear sets. The first planetary gear set- has one 32-sun gears, three 40-planet gears and a stationary 112-tooth ring gear, while the second one has one 28-sungears, three 34-planetgears and a stationary 96-tooth ring gear. Both the ring gears are splined to the top of the transmission casing. The rotating planet gears drive the carrier, which is attached to the output shaft. The output shaft of the planetary gearbox is attached to the spur gear box. The third system is a two-stage spur gearbox.

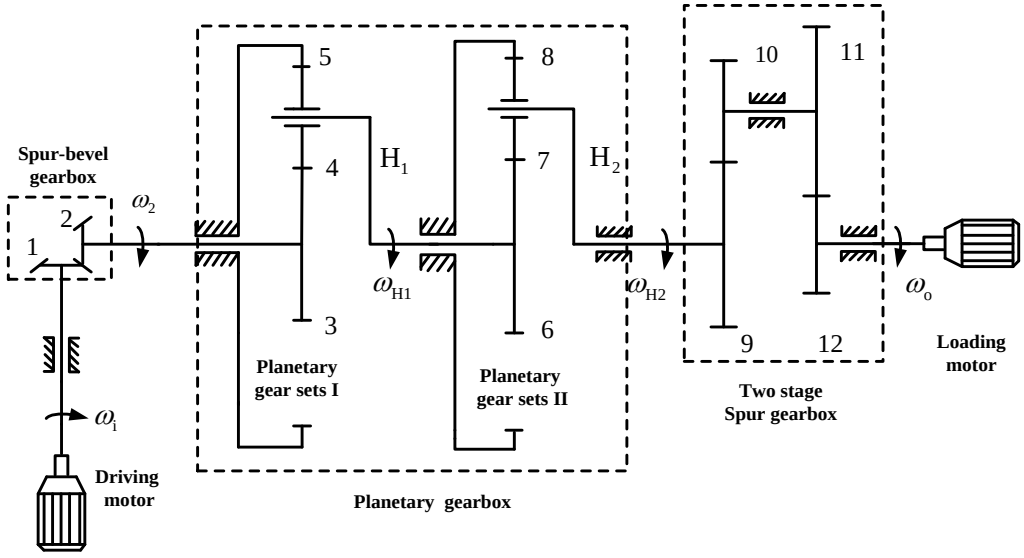

Fig. 5. Helicopter transmission test rig.

5.2. Validation with Test Data

Before the validation with test data, feature selection and weighting have been carried out with simulation signals from dynamical models. The feature selection results show that only a few very features are kept and used in this study. Because there is no prior knowledge of setting the threshold, a median value is used as selection criteria, which resulted in [20, 10, 1] to be the threshold. As shown in Fig.6, the values of z_i s_i and r_i for feature parameters #11, #25 and #27 are above corresponding thresholds and have been selected to be the subset features. These features are FM4, SK and NSR and they are denoted as F1, F2 and F3 respectively in this paper for convenience. Following the procedure to calculate weight values, it has obtained that 0.1283, 0.2509 and 0.6208 are the weights of F1, F2 and F3 respectively, which shows that NSR plays a much more effect on estimating the damage levels.

A number of faults seeded experiments have been conducted in this research. Referring to Fig.7, the test rig consists of two electrical motors, a pair of spur-bevel gears, a planetary gearbox, two pairs of spur gears, a power supply unit with the necessary speed control electronics and the data acquisition system. The characteristics of the planetary gear sets are given in Table 1. The vibration signal generated by the planetary gearbox was picked up by an accelerometer bolted on the top of the planetary gearbox casing and the electrical signal was transferred to the data acquisition system, which has a fore-charge-amplifier. The sampling frequency f_s is 10 kHz. The signal was low-pass filtered at 5 kHz through a 4th order Bessel type filter, in order to limit aliasing distortion and retain waveform integrity as much as possible. Data was stored for post processing to a PC. A number of 10240 data points have been acquired in all experiments corresponding to a time-history length of 1s.

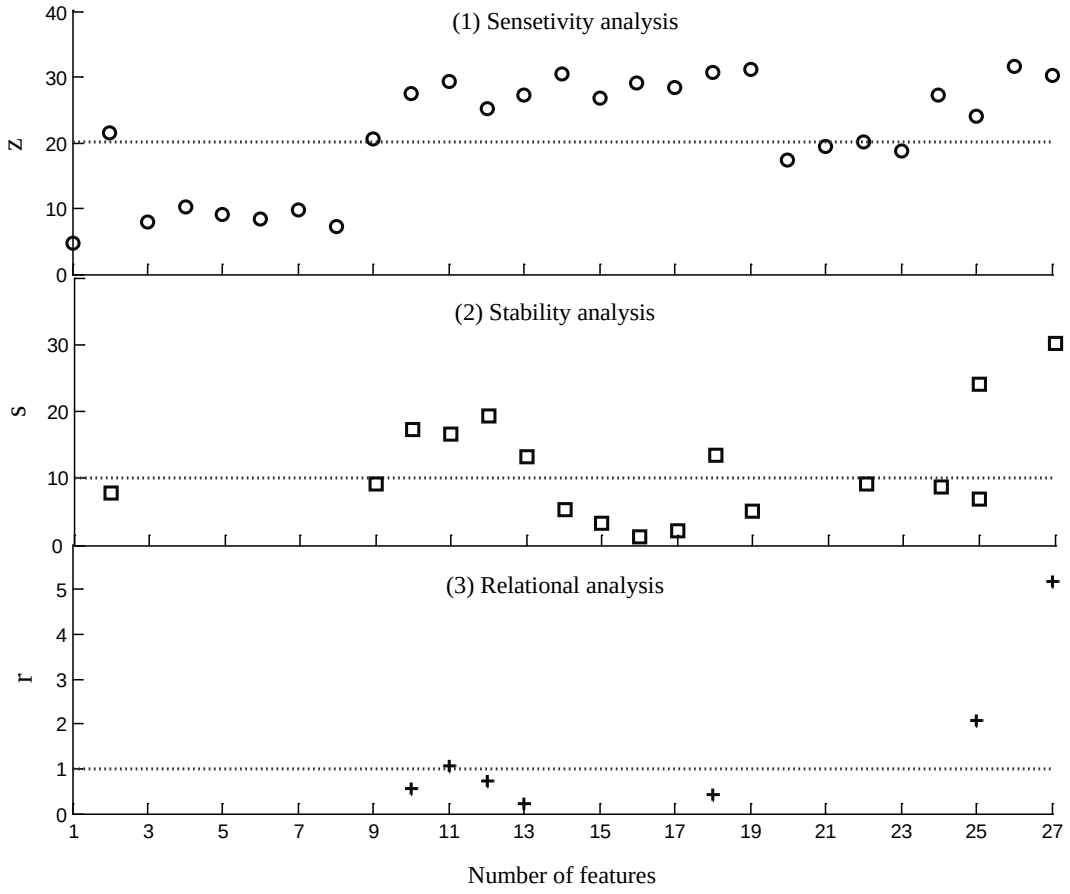

Fig. 6. Feature selection results.

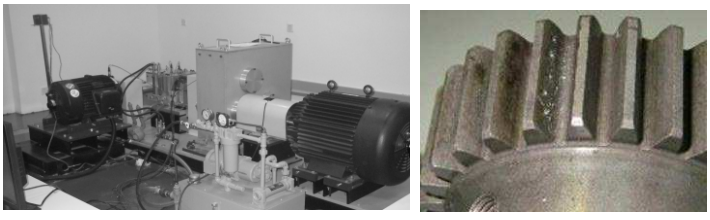

(a) (b)

Fig. 7. Configuration of (a) test rig, and (b) sun-gear with pitting.

To validate the approach in this research, 6 test data {S_1, S_2, S_{x1}, S_{x2}, S_{x3}, S_{x4}} were selected to be analyzed. S_1 and S_2 are the test signals of which damage levels are 0% and 100%, while the other signals' damage levels are unknown. S_1 and S_2 are used to calibrate and normalize feature vectors. We extracted 20 samples from each signal, and calculated the means of features for each sample.

Fig. 8 depicts the damage level estimation results of test data. It can be shown that Test1, Test2, Test3 and Test4 are corresponding to the related damage levels L_3[20%，30%], L_1[0%，10%], L_6[50%，60%], L_8[70%，80%]. To confirm the precision of these results, we checked the test record and obtained the damage levels of the 4 test signals above as s1=25%, s2=0%, s3=53%, s4=77.5%. These records correlate well with the results of damage level estimation.

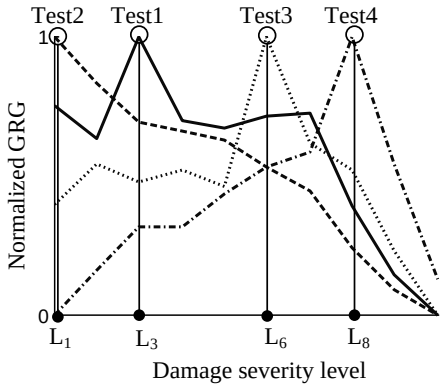

Fig. 8. Damage level estimation results of test data.

6. CONCLUSIONS

In this paper, a new methodology has been developed to estimate the damage severity of 2K-H planetary gear set. The proposed method is firstly calibrated with fault seeded test data and then validated with the data of other tests. The damage level estimation results of test data agree with the actual test records. It has demonstrated the potential of the hybrid models in providing an effective technique to improving the performance of health monitoring and condition prediction.

ACKNOWLEDGEMENTS

This research is supported by the National Natural Sciences Foundation of China (Grant Number 50905183). Valuable comments on the paper from anonymous reviewers are very much appreciated.

REFERENCES

1. Coppe, A. and etc. "A Statistical Model for Estimating Probability of Crack Detection," *2008 International conference on PHM*, CA, USA, Oct. 2008.
2. Choi, S. and Li, C., "Estimation of Gear Tooth Transverse Crack Size from Vibration by Fusing Selected Gear Condition Indices," *Measurement Science and Technology*, Vol. 17, pp. 2395-2400, 2006.
3. Ma, J. and Li, C., "Gear Defect Detection through Model-Based Wideband Demodulation of Vibrations," *Mechanical Systems and Signal Processing*, Vol. 10, No. 5, pp. 653-665, 1996.

4. Lei, Y. and Zuo, M., "Gear Crack Level Identification Based on Weighted K Nearest Neighbor Classification Algorithm," *Mechanical Systems and Signal Processing*, Vol. 23, No. 6, pp. 1535-1547, 2009.
5. Pimsarn, M., Kazerounian, K., "Efficient evaluation of spur gear tooth mesh load using pseudo-interference stiffness estimation method," *Mechanism and Machine Theory*, pp. 769–786, 2002.
6. Wang, J., "Numerical and experimental analysis of spur gears in mesh," PhD, *Curtin University of Technology*, 2003.
7. Ambarisha, V., Parker, R., "Nonlinear dynamics of planetary gears using analytical and finite element models," *Journal of Sound and Vibration*, Vol. 302, pp. 577-595, 2007: pp. 577-595.
8. Lin, J., Parker, R., "Sensitivity of Planetary Gear Natural Frequencies and Vibration on Modes to Model Parameters," *Journal of Sound and Vibration*, Vol. 228, No. 1, pp. 109-128, 1999.
9. Chaari, F., Fakhfakh, T., Haddar, M., "Dynamic analysis of a planetary gear failure caused by tooth pitting and cracking," *Journal of Failure Analysis and Prevention*, Vol. 2, pp. 39–44, 2006.
10. Chaari, F. and Baccar, W., "Effect of Spalling or Tooth Breakage on Gearmesh Stiffness and Dynamic Response of a One-stage Spur Gear Transmission," *European Journal of Mechanics A/Solids*, Vol. 27, No. 4, pp. 691-705, 2008.
11. Hbaieb, R., Chaari, F., Fakhfakh, T., Haddar, M., "Influence of eccentricity, profile error and tooth pitting on helical planetary gear vibration," *Machine Dynamics Problems*, Vol. 29, pp. 5–32, 2005.
12. Walha, L., Louati, J., Fakhfakh, T., Haddar, M., "Dynamic response of two stages gear system damaged by teeth defects," *Machine Dynamics Problems*, Vol. 29, pp. 107–124, 2005.
13. Choy, F., Polychuk, V., Zakarajsek, J., Handschuh, R., Townsend, D., "Analysis of the effects of surface pitting and wear on the vibrations of a gear transmission system," *Tribology*. Vol. 29, pp. 77–83, 1996.
14. Yuksel, C., Kahraman, A., "Dynamic Tooth Loads of Planetary Gear Sets Having Tooth Profile Wear," *Mechanism and Machine Theory*, Vol. 39, pp. 695-715, 2004.
15. Dempsey, P., Lewicki, D., Le, D., "Investigation of Current Methods to Identify Helicopter Gear Health," *2007 IEEE Aerospace Conference*, Big Sky, Montana, March 3-10, 2007.
16. Samuel, P., Pines, D., "A Review of Vibration-based Techniques for Helicopter Transmission Diagnostics," *Journal of Sound and Vibration*, Vol. 282, pp. 475-508. 2005.
17. Lin, J., Zuo, M., "Gearbox fault diagnosis using adaptative wavelet filter," *Mechanical System and Signal Processing*. Vol. 17, pp. 1259–1269, 2003.
18. Saxena, A., Wu, B., Vachtsevanos, G., "A Methodology for Analyzing Vibration Data from Planetary Gear Systems using Complex Morlet Wavelets," *2005 American Control Conference*, Portland, OR, USA, June 8-10, 2005.
19. Wu, B., Saxena, A., "An Approach to Fault Diagnosis of Helicopter Planetary Gears," *2004 IEEE Autotestcon*, pp. 475-481, Sept. 20-23, 2004.
20. Barszcz, T., Randall, R., "Application of Spectral Kurtosis for Detection of a Tooth Crack in the Planetary Gear of a Wind Turbine," *Mechanical Systems and Signal Processing*, Vol. 23, No. 5, pp. 1352-1365, 2009.
21. Antoni, J., Randall, R., "The Spectral Kurtosis: Application to the Vibratory Surveillance and Diagnostics of Rotating Machines," *Mechanical Systems and Signal Processing*, Vol. 20, No. 2, pp. 308-331, 2006.
22. Cheng, Z., Hu, N., Qin, G., "A New Feature for Monitoring of Planetary Gear Sets Based on Physical Model," *Proceedings of the 23rd International Congress on Condition Monitoring and Diagnostic Engineering Management*, Nara, Japan, pp. 289-296, June 28-July 2, 2010.
23. Cheng, Z., Hu, N., Feng, Z., Gao, J., "Detection of Damage in Planetary Gear Sets Based on Dynamical Simulation," *Journal of Vibration Measurement & Diagnosis*, Vol. 30, No. 4, pp. 379-383, 2010.

APPENDIX

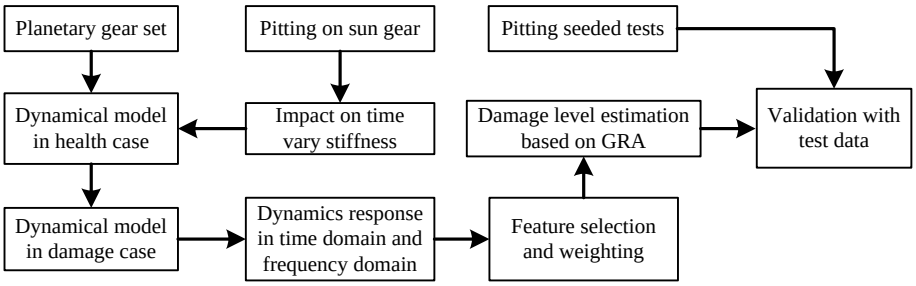

Flow chart of the research